

Hydrogen atom in a magnetic field: electromagnetic transitions of the lowest states

J.C. López Vieyra and H.O. Pilón
Instituto de Ciencias Nucleares, UNAM,
Apartado Postal 70-543, 04510 México,
e-mail: vieyra@nucleares.unam.mx, horop@nucleares.unam.mx

Recibido el 29 de septiembre de 2007; aceptado el 5 de diciembre de 2007

A detailed study of the lowest states $1s_0, 2p_{-1}, 2p_0$ of the hydrogen atom placed in a magnetic field $B \in (0 - 4.414 \times 10^{13} \text{ G})$ and their electromagnetic transitions ($1s_0 \leftrightarrow 2p_{-1}$ and $1s_0 \leftrightarrow 2p_0$) is carried out in the infinite-proton-mass (Born-Oppenheimer) approximation. The variational method is used with a physically motivated recipe to design simple trial functions applicable to the whole domain of magnetic fields. We show that the proposed functions yield very accurate results for the ionization (binding) energies. Dipole and oscillator strengths are in good agreement with results by Ruder *et al.* [10], although we observe deviations of up to $\sim 30\%$ for the oscillator strength of the linearly polarized electromagnetic transition $1s_0 \leftrightarrow 2p_0$ at strong magnetic fields $B \gtrsim 1000 \text{ a.u.}$

Keywords: hydrogen atom; magnetic fields; transitions.

Se lleva a cabo un estudio detallado de los estados más bajos $1s_0, 2p_{-1}, 2p_0$ del átomo de hidrógeno en un campo magnético $B \in (0 - 4.414 \times 10^{13} \text{ G})$ y sus transiciones electromagnéticas ($1s_0 \leftrightarrow 2p_{-1}$ and $1s_0 \leftrightarrow 2p_0$) en la aproximación de masa del protón infinita (Born-Oppeneimer). Se usa el método variacional con una receta físicamente motivada para diseñar funciones de prueba simples aplicables a el rango completo de campos magnéticos. Mostramos que las funciones propuestas arrojan resultados muy precisos para las energías de ionización (energías de amarre). Las fuerzas de dipolo y de oscilador estan en buen acuerdo con los resultados de Ruder *et al.* [10] aunque observamos desviaciones de hasta $\sim 30\%$ para la fuerza de oscilador de la transición electromagnética linealmente polarizada $1s_0 \leftrightarrow 2p_0$ para campos magnéticos $B \gtrsim 1000 \text{ a.u.}$

Descriptores: átomo de hidrógeno; campos magnéticos; transiciones.

PACS: 31.15.Pf; 31.10.+z; 32.60.+i; 97.10.Ld

1. Introduction

Contemporary X-ray space observatories, such as Chandra, XMM-Newton and their predecessors, have collected a considerable amount of observational data of the thermal emission coming from surface layers of neutron stars, which are characterized by enormous magnetic fields $B \sim 10^{12} - 10^{13} \text{ G}$ (see *e.g.* Refs. 1 and 2). In particular, the observation of absorption features in the X-ray spectrum of some isolated neutron stars (see *e.g.* Refs. 3 and 4) has suggested possible models of atmospheres which allow the presence of Coulomb systems [5–8]. The hydrogen atom is the simplest and most studied Coulombic system in weak and strong magnetic fields (see for example the early review Ref. 9 and references therein, and Refs. 10 to 12 for more recent studies).

In the present study our goal is to apply a physics recipe (described in full generality in Ref. 13) for choosing variational trial functions to study the hydrogen atom in a magnetic field and its electromagnetic transitions between the lowest bound states $1s_0, 2p_{-1}$ and $2p_0$. The study is intended as a test of the methodology developed in Ref. 13. Electromagnetic transitions in the hydrogen atom in the absence of a magnetic field constitute a widely described subject (see *e.g.* Ref. 14). In a strong magnetic field, such electromagnetic transitions have been studied by a number of authors (see *e.g.* Ref. 10 and 15). Special interest has been given to the

study of the center-of-mass effects on the transition probabilities due to the transverse motion across the magnetic field direction (see *e.g.* Refs. 16 to 19, and 20 —for the case of the He^+ atomic-ion).

Our consideration is non-relativistic, based on a variational solution of the Schrödinger equation. Thus, the magnetic field strength is restricted by the Schwinger limit $B = 4.414 \times 10^{13} \text{ G}$. Our study is also based on the Born-Oppenheimer approximation of zero order: the proton is assumed to be infinitely massive. Thus we neglect the effects of the CM motion, *i.e.* the effects of the transverse motion of the atom with respect to the magnetic field orientation. The study is realized in two steps:

- (i) a variational calculation of the states $1s_0, 2p_{-1}$ and $2p_0$ is done with suitable trial functions (selected according to the physics recipe), and
- (ii) with the variationally obtained approximate wavefunctions we calculate the allowed radiative transitions among these states in the electric dipole approximation (see below).

Atomic units are used throughout ($\hbar=m_e=e=1$), albeit energies are expressed in Rydberg (Ry). The magnetic field B is given in a.u. with $B_0 = 2.35 \times 10^9 \text{ G}$, although frequently we will also use magnetic fields strengths given in Gauss for convenience.

1.1. Hamiltonian

The Hamiltonian which describes the Coulomb system formed by an infinitely massive proton and one electron (pe) placed in a homogeneous constant magnetic field directed along the z -axis, $\mathbf{B} = (0, 0, B)$, is given by

$$\hat{\mathcal{H}} = (\hat{\mathbf{p}} + \mathcal{A})^2 - \frac{2}{r} = \hat{\mathbf{p}}^2 - \frac{2}{r} + (\hat{\mathbf{p}} \cdot \mathcal{A} + \mathcal{A} \cdot \hat{\mathbf{p}}) + \mathcal{A}^2, \quad (1)$$

where $\hat{\mathbf{p}} = -i\nabla$ is the electron momentum, r is the distance between the electron and the proton fixed at the origin, and \mathcal{A} is a vector potential corresponding to the magnetic field \mathbf{B} . A contribution to the energy coming from the coupling between the electron intrinsic magnetic moment and the magnetic field $\sim \hat{\mathbf{S}} \cdot \mathbf{B}$, being constant, has been dropped from (1). Now, if we choose the vector potential in the symmetric gauge

$$\mathcal{A} = \frac{B}{2}(-y, x, 0),$$

the Hamiltonian acquires the form

$$\hat{\mathcal{H}} = -\Delta - \frac{2}{r} + \hat{l}_z B + \frac{B^2 \rho^2}{4}, \quad (2)$$

where Δ is the Laplacian operator, and \hat{l}_z is the conserved z -component of the electron angular momentum. The Hamiltonian (2) is also invariant with respect to the z -parity π_z (*i.e.* reflections $z \rightarrow -z$). Thus the eigenstates can be classified

by (m, π_z) : the magnetic quantum number m , corresponding to the conservation of \hat{l}_z , and the z -parity quantum number $\pi_z = \pm 1$. From here on, we shall use the field-free notation $1s_0, 2p_{-1}, 2p_0$, to denote the lowest states with quantum numbers $(m, \pi_z) = (0, +), (-1, +), (0, -)$, respectively.

1.2. Choice of trial functions

The procedure which we use to explore the problem is the variational method with a well defined recipe for choosing trial functions. This recipe is based on physical arguments, described in full generality in Ref. 13. The basic ingredients are

- (i) for a given trial function ψ_{trial} , the potential $V_{trial} = \Delta\psi_{trial}/\psi_{trial}$, for which said function is an exact eigenfunction, should reproduce as many as possible the basic properties of the original potential, *e.g.* in the present case it should reproduce the Coulomb singularities and the harmonic oscillator behavior at small and large r distances respectively, and (
- ii) the trial function ψ_{trial} should include the symmetries of the problem. For example, if the ground state is studied, the trial function ψ_{trial} must be a nodeless function.

Adhering to this recipe, in Ref. 21 the following function was proposed for the hydrogen ground state $1s_0$:

$$\Psi_{1s_0} = e^{-\sqrt{\gamma_1 r^2 + (\gamma_2 r^3 + \gamma_3 \rho^2 r + \gamma_4 \rho^3 + \gamma_5 \rho r^2) B^2 + \frac{\gamma_6 B^2 \rho^4}{16} + \frac{\gamma_7 B^2 \rho^2 r^2}{16}}}, \quad (3)$$

where $\gamma_1, \dots, \gamma_7$ are variational parameters. The potential associated with function (3) reproduces the Coulomb singularity at $r \rightarrow 0$ as well as the harmonic oscillator for $r \rightarrow \infty$ of the original Hamiltonian (2). Function (3) has no nodes. From here on, we shall use function (3) for the variational study of the ground state $1s_0$.

For the lowest excited states $2p_{-1}, 2p_0$ the presence of the magnetic field does not modify the nodal structure of the field-free exact eigenfunctions[†]. A hint for this can be obtained in first order degenerate perturbation theory in B^2 , where one can see that the states $2p_{-1}, 2p_0$ are not mixed. Thus the following variational functions for the $2p_{-1}, 2p_0$ states are proposed:

$$\Psi_{2p_{-1}} = \rho e^{-i\phi} \psi_0, \quad (4)$$

$$\Psi_{2p_0} = z \psi_0, \quad (5)$$

where the functions ψ_0 have the same functional form as (3) but with their own γ -parameters. Thus, in functions (4), (5), we keep the same polynomial prefactor as in the corresponding field-free wavefunctions and multiply them by a nodeless function. It is easy to check that the functions (3), (4)

and (5) are orthogonal. These functions will describe the lowest energy states among the states with quantum numbers $(m, \pi_z) = (0, +), (-1, +), (0, -)$ ($1s_0, 2p_{-1}, 2p_0$, respectively) in the entire range of magnetic fields studied.

2. Electromagnetic transitions

In a magnetic field, the m -degeneracy of the hydrogen energy levels is fully removed and electromagnetic transitions depend explicitly on the magnetic quantum numbers of the initial and final states in the transition. A consideration of electromagnetic transitions in the electric dipole approximation is valid even in the case of high magnetic fields, as long as transitions occur among states with the same Landau quantum number; in this case the characteristic wave lengths are always much larger than the (longitudinal or transverse) *size* of the system (for a discussion on the validity of the dipole approximation see *e.g.* Refs. 10 and 16). All the states considered in the present study belong to the same ground Landau-level and thus the electric dipole approximation is justified.

Relevant formulas for the electromagnetic transitions in the hydrogen atom in a magnetic field were given in Ref. 15. In the electric dipole approximation, we are interested in the square of the matrix element (called dipole strength)

$$d_{\tau',\tau}^{(q)} = |p_{\tau',\tau}^{(q)}|^2 = |\langle \tau' | r^{(q)} | \tau \rangle|^2, \quad (6)$$

where τ', τ label the final and initial states in the transition, and $r^{(q)}$ ($q = 0, \pm 1$) are the spherical components of the electric dipole operator. The oscillator strength of the transition is given by

$$f_{\tau',\tau}^{(q)} = (E_b^{\tau'} - E_b^\tau) |p_{\tau',\tau}^{(q)}|^2, \quad (7)$$

where $(E_b^{\tau'} - E_b^\tau)$ is the (binding) energy difference of the initial and final states. The transition probability is calculated according to the relation

$$w_{\tau',\tau}^{(q)} = \frac{1}{3\tau_0} (E_b^{\tau'} - E_b^\tau)^3 |p_{\tau',\tau}^{(q)}|^2, \quad (8)$$

where $1/\tau_0 = 8.03 \times 10^9 \text{ sec}^{-1}$. We have two selection rules implicit in the matrix element $p_{\tau',\tau}^{(q)}$ (Eq. (6)) *viz.*, parity change and

$$\Delta m = 0, \pm 1, \quad (9)$$

which implies $q = \Delta m$. Thus, the transitions with $\Delta m = 0$ are characterized by a linearly polarized radiation along the magnetic field direction with $q = 0$, while the transitions with $\Delta m = 1$ are characterized by circularly polarized radiation with $q = +1$ (for right polarization), or $q = -1$ (for left polarization).

3. Results

3.1. Binding Energies

The results of the variational calculations of the total (E_T) and bindingⁱⁱ (E_b) energies for the lowest $1s_0$, $2p_{-1}$ and $2p_0$ states of the hydrogen atom in a magnetic field ranging $0.235 \times 10^9 \text{ G} \leq B \leq 4.414 \times 10^{13} \text{ G}$ are presented in Tables I, II and III, respectivelyⁱⁱⁱ. Results for binding energies of these lowest states are also summarized in Fig. 1. In this figure, one can immediately see that the binding energy grows steadily as the magnetic field increases for all three states $1s_0$, $2p_{-1}$ and $2p_0$. In particular, the ionization energy reaches $\sim 0.4 \text{ keV}$ for a magnetic field at the Schwinger limit, where $B = 4.414 \times 10^{13} \text{ G}$. The increase in binding energy as the magnetic field grows is *faster* (and comparable) for the bound states $1s_0$, and $2p_{-1}$ (increasing ~ 20 times for the domain $B \sim 10^9 - 10^{13} \text{ G}$) as compared with the rate of increase of the binding energy for the bound state $2p_0$ (increasing only ~ 2 times for the domain $B \sim 10^9 - 10^{13} \text{ G}$). In fact the binding energy of the state $2p_0$ approaches the value $E_b = 1 \text{ Ry}$ as $B \rightarrow \infty$ (see Ref. 22 and Table III).

For all states studied, the results of the binding energies given by the simple trial functions (3), (4), (5) are, in general, in very good agreement with the adiabatic approach of Ruder *et al.* [10] (where a basis expansion in terms of spherical harmonics is used for the weak field regime and in terms of Landau states for the strong field regime) and with the highly accurate approach of Kravchenko *et al.* [11] (where a power series expansion of the eigenfunctions is used).

TABLE I. Total E_T and binding E_b energies for the ground state $1s_0$ of the hydrogen atom in a magnetic field calculated with the variational function (3) compared with the results obtained by Ruder *et al.* [10] and Kravchenko *et al.* [11]. The values of the energies have been rounded to the first two non-coinciding digits with respect to the values in Ref. 11.

$B \times 10^9 \text{ G}$	Variational calculation		Ref. 10	Ref. 11
	E_T (Ry)		E_b (Ry)	
0.235	-0.99505296	1.09505296 ^a	1.095053	1.09505296
1.0	-0.9208225	1.3463544 ^a	-	-
2.35	-0.662332	1.662332 ^a	1.662338	1.66233779
10.0	1.640362	2.614957 ^a	-	-
23.5	6.50522	3.4948 ^a	3.495594	3.49559433
100.0	36.8398	5.7134 ^a	-	-
235.0	92.4356	7.564 ^a	7.5781	7.57960847
1000.0	413.662	11.870 ^a	-	-
2350.0	984.773	15.23 ^a	15.3241	15.32484649
10000.0	4232.77	22.55 ^a	-	-
23500.0	9972.0	27.96	-	-
44140.0	18750.5	32.5 ^a	-	-

^aResults of Ref. [21].

TABLE II. Total E_T and binding E_b energies for the state $2p_{-1}$ of the hydrogen atom in a magnetic field as given by the trial function (4) compared with the results obtained by Ruder *et al.* [10] and Kravchenko *et al.* [11]. The values of the energies have been rounded to the first two non-coinciding digits with respect to the values in Ref. 11.

$B \times 10^9 G$	Variational Calculations		Ref. 10	Ref. 11
	E_T (Ry)		E_b (Ry)	
0.235	-0.3016912	0.40169120	0.4016913	0.40169135
1.0	-0.232205	0.657737	-	-
2.35	0.08684	0.913163	0.9131941	0.91319412
10.0	2.64128	1.6140	-	-
23.5	7.75028	2.2497	2.250845	2.25084468
100.0	38.6802	3.873	-	-
235.0	94.744	5.256	5.26948	5.26952133
1000.0	416.975	8.557	-	-
2350.0	988.80	11.20	11.27681	11.27684216
10000.0	4238.22	17.10	-	-
23500.0	9978.44	21.56	-	-
44140.0	18757.6	25.4	-	-

TABLE III. Total E_T and binding E_b energies for the state $2p_0$ of the hydrogen atom in a magnetic field as given by the trial function (5) compared with the results obtained by Ruder *et al.* [10] and Kravchenko *et al.* [11]. The values of the energies have been rounded to the first two non-coinciding digits with respect to the values in Ref. 11.

$B \times 10^9 G$	Variational Calculations		Ref. 10	Ref. 11
	E_T (Ry)		E_b (Ry)	
0.235	-0.2248199	0.3248199	0.3248202	0.32482016
1.0	-0.008703	0.434235	-	-
2.35	0.48008	0.5199	0.5200132	0.52001323
10.0	3.5779	0.6774	-	-
23.5	9.2359	0.7641	0.7652975	0.76529970
100.0	41.674	0.8796	-	-
235.0	99.074	0.9255	0.9272354	0.92723552
1000.0	424.561	0.9710	-	-
2350.0	999.016	0.9844	0.9849900	0.9849900
10000.0	4254.33	0.9938	-	-

For small to moderately high magnetic fields ($B \lesssim 1$ a.u.), the relative differences between our binding energies and those of [10, 11] are found to be $\lesssim 10^{-4}$. It is worth emphasizing the remarkable coincidence in 9 digits for the ground state binding energy given by (3) and the most accurate results up to date of Refs. 10 and 11 in the domain of magnetic fields $B \lesssim 0.1$ a.u. The agreement of the binding energies with the corresponding perturbative results

$$E_b^{1s_0} \simeq 1 + B - \frac{1}{2}B^2,$$

$$E_b^{2p_{-1}} \simeq \frac{1}{4} + 2B - 6B^2,$$

$$E_b^{2p_0} \simeq \frac{1}{4} + B - 3B^2,$$

obtained with a logarithmic perturbation theory (see Refs. 13, 23, and 24 and references therein), is also very good.

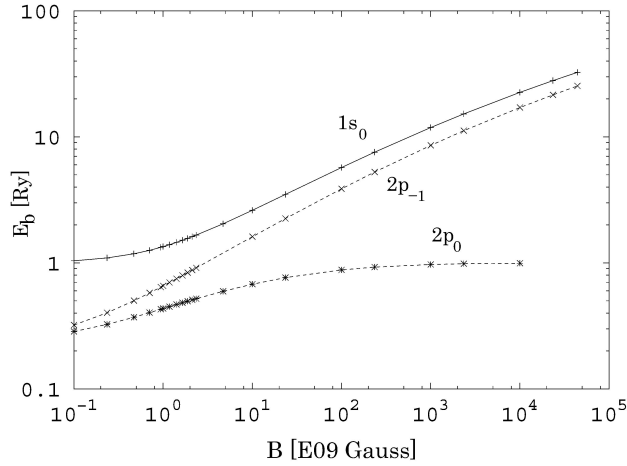


FIGURE 1. Binding energies E_b for the three lower states $1s_0$, $2p_{-1}$, $2p_0$ of the hydrogen atom as functions of magnetic field strength B . The curves show the calculated values of E_b using the variational function (3) for the ground state $1s_0$ (marked by +), the function (4) for the state $2p_{-1}$ (marked by \times), and the function (5) for the state $2p_0$ (marked by *). The points corresponding to the same state are joined by line segments.

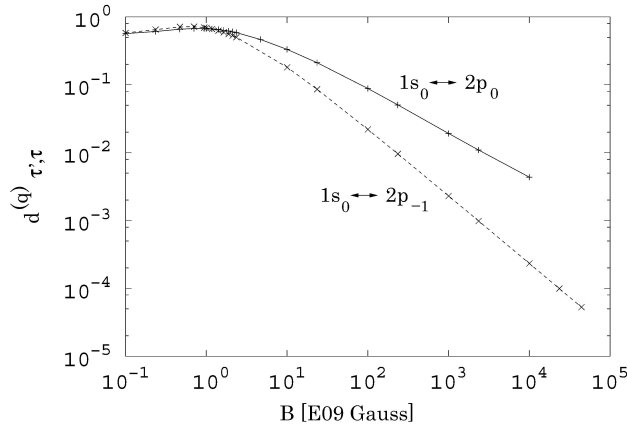


FIGURE 2. Dipole strengths $d_{\tau,\tau}^{(q)}$ for the transitions $1s_0 \leftrightarrow 2p_{-1}$, and $1s_0 \leftrightarrow 2p_0$ as functions of magnetic field strength B . The curves show the calculated values of the dipole strengths $d_{1s_0 \leftrightarrow 2p_{-1}}^{(+1)}$ (marked by \times) and $d_{1s_0 \leftrightarrow 2p_0}^{(0)}$ (marked by +) joined by line-segments.

However, the results for the binding energies of the three states studied, obtained with the variational functions (3), (4) and (5), show that the accuracy gradually decreases as the magnetic field increases and the relative differences for such binding energies (when compared with the corresponding results of Refs. 10 and 11) reach values of $\sim 10^{-2}$ for $B \gtrsim 1000$ a.u. (see Tables I, II, III). It indicates that the adiabatic separation of the transverse and longitudinal degrees of freedom is slightly delayed in functions (3), (4) and (5).

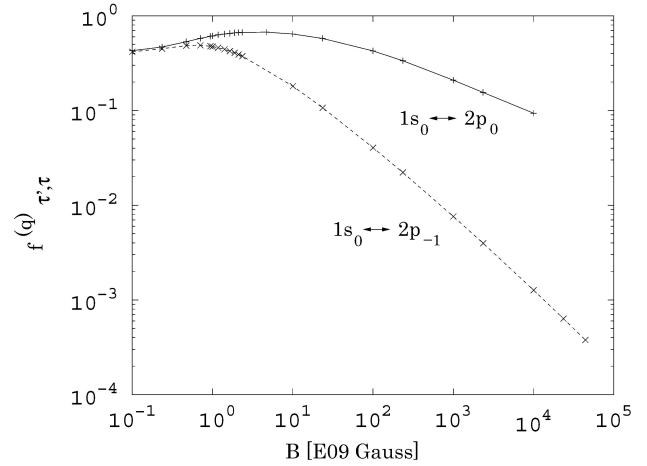


FIGURE 3. Oscillator strengths $f_{\tau,\tau}^{(q)}$ for the transitions $1s_0 \leftrightarrow 2p_{-1}$, and $1s_0 \leftrightarrow 2p_0$ as functions of magnetic field strength B . The curves show the calculated values of the oscillator strengths $f_{1s_0 \leftrightarrow 2p_{-1}}^{(+1)}$ (marked with the symbol \times) and $f_{1s_0 \leftrightarrow 2p_0}^{(0)}$ (marked with the symbol +) joined by line-segments.

A comparison of the binding energies of the two lowest states $1s_0$ ($m = 0$) and $2p_{-1}$ ($m = -1$) with the asymptotic (adiabatic) formulas

$$E_b^{(m)} \simeq \log^2 \frac{B}{\sqrt{2|m|+1}}$$

(see *e.g.* [11]) shows that, in both cases, the results given by this asymptotic formula are still far from the more accurate variational calculations, differing by a factor of about 3 for the highest magnetic fields studied. For instance, for the magnetic field $B = 10000$ a.u., the adiabatic formula gives $E_b^{1s_0} \simeq 85$ Ry and $E_b^{2p_{-1}} \simeq 75$ Ry, while the present numerical results are $E_b^{1s_0} = 27.96$ Ry and $E_b^{2p_{-1}} = 21.56$ Ry, respectively (see Tables I, II). Even the asymptotic binding energy difference $\Delta E_b^{\text{asympt}} \simeq 9.8$ Ry is about 1.5 times larger than the variational one, $\Delta E_b^{\text{var}} \simeq 6.4$ Ry, for such magnetic field strength.

In practice, a full variational calculation is easily done on a standard desktop computer; it takes very few minutes of CPU time.

3.2. Transitions

With the approximate wavefunctions (3), (4) and (5) found in the variational procedure described above, we carried out a study of the electromagnetic transitions between states $2p_{-1}$, $2p_0$ and the ground state $1s_0$, *i.e.* $1s_0 \leftrightarrow 2p_{-1}$ ($\Delta m = 1$), and $1s_0 \leftrightarrow 2p_0$ ($\Delta m = 0$). The transition $1s_0 \leftrightarrow 2p_{-1}$ occurs by absorption (emission) of circular-right-polarized radiation ($q = +1$), while the transition $1s_0 \leftrightarrow 2p_0$ occurs by absorption (emission) of linearly-polarized (along the magnetic field direction) radiation ($q = 0$). Neither $2p_{-1}$ nor $2p_0$ have an excitation (de-excitation) mode to the ground state via left-polarized radiation.

The first remarkable observation concerning the electromagnetic transitions is the fact that, if for small magnetic

fields the transition probabilities for both transitions are comparable in magnitude, for strong magnetic fields the (circularly polarized) transition $1s_0 \leftrightarrow 2p_{-1}$ is strongly suppressed in comparison to the corresponding transition probability for the (linearly polarized) transition $1s_0 \leftrightarrow 2p_0$ (see Fig. 4). This phenomenon is a consequence of the strong deformation of the electronic distribution due to the enormous Lorentz force acting on it, being elongated in the direction of the magnetic field, thus enhancing the longitudinal polarization transition mode $q = 0$ with respect to the transverse transition modes $q = \pm 1$.

At the other extreme of small magnetic fields, perturbative results for the dipole and oscillator strengths and transi-

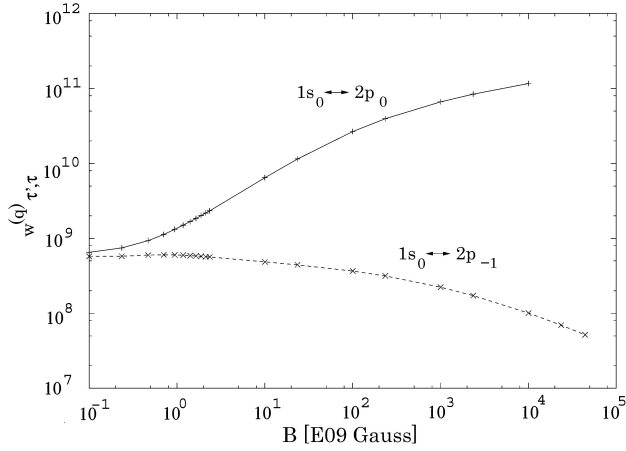


FIGURE 4. Transition probabilities $w_{\tau, \tau}^{(q)}$ for the transitions $1s_0 \leftrightarrow 2p_{-1}$, and $1s_0 \leftrightarrow 2p_0$. The curves show the calculated values of the transition probabilities $w_{1s_0 \leftrightarrow 2p_{-1}}^{(+1)}$ (marked with the symbol \times) and $w_{1s_0 \leftrightarrow 2p_0}^{(0)}$ (marked with the symbol $+$) joined by line-segments.

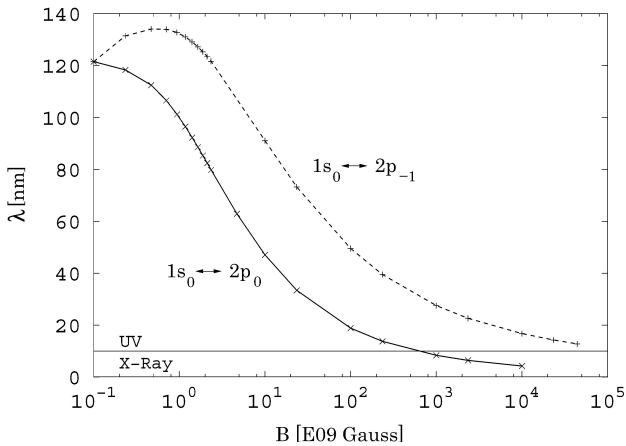


FIGURE 5. Wavelengths of (a) the right-circular polarized radiation associated with the transition $1s_0 \leftrightarrow 2p_{-1}$ (dashed curve) and (b) of the linearly polarized radiation associated with the transition $1s_0 \leftrightarrow 2p_0$ (solid curve), as functions of the magnetic field B . The curves show the calculated values of the wavelengths $\lambda_{1s_0 \leftrightarrow 2p_{-1}}$ (marked with the symbol $+$) and $\lambda_{1s_0 \leftrightarrow 2p_0}$ (marked with the symbol \times) joined by line-segments.

tion probabilities are given by [24]:

$$d_{1s_0 \leftrightarrow 2p_{-1}}^{(+1)} \simeq 0.555 + 29.776B^2,$$

$$f_{1s_0 \leftrightarrow 2p_{-1}}^{(+1)} \simeq 0.416 - 0.555B + 25.841B^2,$$

$$w_{1s_0 \leftrightarrow 2p_{-1}}^{(+1)} \simeq (6.266 - 25.066B + 171.280B^2) \times 10^8 \text{ sec}^{-1},$$

for the $1s_0 \leftrightarrow 2p_{-1}$ transition, and

$$d_{1s_0 \leftrightarrow 2p_0}^{(0)} \simeq 0.555 + 9.388B^2,$$

$$f_{1s_0 \leftrightarrow 2p_0}^{(0)} \simeq 0.416 + 8.428B^2,$$

$$w_{1s_0 \leftrightarrow 2p_0}^{(0)} \simeq (6.266 + 126.894B^2) \times 10^8 \text{ sec}^{-1},$$

for the $1s_0 \leftrightarrow 2p_0$ transition, where the magnetic field strength B is in a.u. These results show different behaviors for both transitions. While for the $1s_0 \leftrightarrow 2p_0$ transition all quantities $d_{1s_0 \leftrightarrow 2p_0}^{(0)}$, $f_{1s_0 \leftrightarrow 2p_0}^{(0)}$ and $w_{1s_0 \leftrightarrow 2p_0}^{(0)}$ are growing functions of B^2 , in the case of the $1s_0 \leftrightarrow 2p_{-1}$ transition the oscillator strength $f_{1s_0 \leftrightarrow 2p_{-1}}^{(+1)}$ and the transition probability $w_{1s_0 \leftrightarrow 2p_{-1}}^{(+1)}$ slightly decrease for small increasing magnetic fields, reaching a minimum for $B \simeq 10^{-2}$ a.u. and $B \simeq 10^{-1}$ a.u., respectively. For larger magnetic fields $B \sim 10^{-1}$ a.u., all quantities $d_{1s_0 \leftrightarrow 2p_0}^{(0)}$, $f_{1s_0 \leftrightarrow 2p_0}^{(0)}$, $w_{1s_0 \leftrightarrow 2p_0}^{(0)}$ and $d_{1s_0 \leftrightarrow 2p_{-1}}^{(+1)}$, $f_{1s_0 \leftrightarrow 2p_{-1}}^{(+1)}$, $w_{1s_0 \leftrightarrow 2p_{-1}}^{(+1)}$ are growing functions of B^2 . As we go to higher (non-perturbative) magnetic fields, the results obtained with the variational functions (3), (4) and (5) show that the dipole strengths and the oscillator strengths of both transitions eventually reach a maximum as the magnetic field grows, after which they start to decrease monotonously in the region of high magnetic fields $B \gtrsim 1$ a.u. For the $1s_0 \leftrightarrow 2p_{-1}$ transition, the maximum in the dipole strength $d_{1s_0 \leftrightarrow 2p_{-1}}^{(+1)}(B)$ and the maximum in the oscillator strength $f_{1s_0 \leftrightarrow 2p_{-1}}^{(+1)}(B)$ approximately coincide at $B \simeq 0.3$ a.u. The transition probability also shows a maximum for the same value magnetic field. In contrast, in the $1s_0 \leftrightarrow 2p_0$ transition, the maximum in the dipole strength $d_{1s_0 \leftrightarrow 2p_0}^{(0)}(B)$ occurs for $B \simeq 0.3$ a.u. but the maximum in the oscillator strength $f_{1s_0 \leftrightarrow 2p_0}^{(0)}(B)$ occurs for $B \simeq 2$ a.u. However, the transition probability $w_{1s_0 \leftrightarrow 2p_0}^{(0)}(B)$ is an increasing function of the magnetic field (Fig. 4).

Our results for $d^{(+1)}$, $f^{(+1)}$, $w^{(+1)}$ corresponding to the $1s_0 \leftrightarrow 2p_{-1}$ transition are in good agreement with the results in Ref. 10 in the whole domain of magnetic fields. The relative differences between our results for the dipole and oscillator strengths and the corresponding results in Ref. 10 are $\sim 10^{-5}$ for magnetic fields $B \sim 0.1$ a.u., increasing rather monotonously when the magnetic field grows being $\sim 10^{-3}$ at $B \sim 1000$ a.u. Our results for the transition probability are also in good agreement with the results in [10], the relative differences to reach $\sim 10^{-4} - 10^{-3}$ for magnetic fields $B \sim 0.1 - 100$ a.u. The largest relative difference $\sim 10^{-2}$ is observed at $B = 1000$ a.u. (see Table II).

Major differences occur in the case of the $1s_0 \leftrightarrow 2p_0$ transition. For instance, the relative differences between present results for the oscillator strengths and the corresponding results in Ref. 10 are $\sim 10^{-4}$ for magnetic fields $B \sim 0.1$ a.u. increasing with a magnetic field increase to reach $\sim 10^{-1}$ at $B \sim 1000$ a.u. The corresponding relative differences for the dipole strength are $\sim 10^{-4}$ for magnetic fields $B \sim 0.1$ a.u. increasing up to ~ 0.3 at $B = 1000$ a.u. A similar deviation is observed in the results for the transition probability for $1s_0 \leftrightarrow 2p_0$ where the relative difference

is $\sim 10^{-4}$ for magnetic fields $B \sim 0.1$ a.u. and increasing up to ~ 0.3 at $B = 1000$ a.u. A possible explanation for the occurrence of such deviations in results of the present calculations and those of Ref. 10 is an apparent delayed adiabatic separation of the transverse and longitudinal degrees of freedom in the trial functions (3), (5) as $B \rightarrow \infty$. However, it is important to emphasize here that there is no criterion for other observables, except in the case of the total (or binding) energy, to determine which values are more accurate^{iv}.

TABLE IV. Results for the electromagnetic transition $1s_0 \leftrightarrow 2p_{-1}$ in the hydrogen atom in a magnetic field B obtained with the variational functions (3) and (4) compared with the results of Ruder *et al.* [10] for the case of infinite nuclear mass. The units for the transition probability are 10^8 sec^{-1} .

$B \times 10^9 G$	Dipole Strength		Oscillator Strength		Transition Probability $w_{1s_0 \leftrightarrow 2p_{-1}}^{(+1)}$	
	$d_{1s_0 \leftrightarrow 2p_{-1}}^{(+1)}$	Ref. 10	$f_{1s_0 \leftrightarrow 2p_{-1}}^{(+1)}$	Ref. 10		Ref. 10
0.0	0.55493		0.41620		6.2664	
0.235	0.64837	0.6484	0.44955	0.4496	5.7849	5.7852
1.0	0.68681	-	0.47295	-	6.0030	-
2.35	0.50133	0.5015	0.37558	0.3757	5.6423	5.6437
10.0	0.18073	-	0.18089	-	4.8509	-
23.5	0.08576	0.08584	0.10678	0.1069	4.4305	4.4313
100.0	0.021987	-	0.04046	-	3.6683	-
235.0	0.009581	0.009591	0.02212	0.02214	3.1552	3.1587
1000.0	0.002296	-	0.00761	-	2.2355	-
2350.0	0.0009837	0.0009847	0.00396	0.003985	1.7231	1.7474
10000.0	0.0002325	-	0.00127	-	1.0068	-
23500.0	0.0000992	-	0.00063	-	0.6950	-
44140.0	0.0000529	-	0.00038	-	0.5165	-

TABLE V. Results for the electromagnetic transition $1s_0 \leftrightarrow 2p_0$ in the hydrogen atom in a magnetic field B obtained with the variational functions (3) and (5) compared with the results of Ruder *et al.* [10] for the case of infinite nuclear mass. The units for the transition probability are 10^8 sec^{-1} .

$B \times 10^9 G$	Dipole Strength		Oscillator Strength		Transition Probability $w_{1s_0 \leftrightarrow 2p_0}^{(0)}$	
	$d_{1s_0 \leftrightarrow 2p_0}^{(0)}$	Ref. 10	$f_{1s_0 \leftrightarrow 2p_0}^{(0)}$	Ref. 10		Ref. 10
0.0	0.55493		0.41620		6.2664	
0.235	0.60843	0.6083	0.46864	0.4685	7.4417	7.4401
1.0	0.67290	-	0.61377	-	13.668	-
2.35	0.58565	0.5902	0.66905	0.6742	23.372	23.549
10.0	0.33129	-	0.64189	-	64.499	-
23.5	0.21101	0.2252	0.57621	0.6149	115.01	122.69
100.0	0.088027	-	0.42551	-	266.12	-
235.0	0.050464	0.06217	0.33502	0.4135	395.24	489.56
1000.0	0.019169	-	0.20893	-	664.29	-
2350.0	0.010898	0.01585	0.15522	0.2273	842.82	1250.81
10000.0	0.0043462	-	0.093697	-	1165.6	-

In the domain of very strong magnetic fields ($B \gtrsim 10^{12}$ G), our results for dipole strengths of both transitions show the approximate scalings $d_{1s_0 \leftrightarrow 2p_0}^{(0)} \sim (B/B_0)^{-2/3}$, and $d_{1s_0 \leftrightarrow 2p_{-1}}^{(+1)} \sim (B/B_0)^{-1}$, accurate to $\lesssim 10\%$ and $\lesssim 1\%$ respectively. Likewise, the results for the oscillator strengths scale approximately as $f_{1s_0 \leftrightarrow 2p_0}^{(0)} \sim \frac{3}{2} (B/B_0)^{-1/3}$, and $f_{1s_0 \leftrightarrow 2p_{-1}}^{(+1)} \sim (B/B_0)^{-4/5}$, both accurate to $\lesssim 5\%$.

Finally, in Fig. 5 we show the wavelengths $\lambda = 2\pi/\alpha (E_b^{\tau'} - E_b^{\tau})$ ($\alpha \simeq 1/137$ is the fine structure constant and $(E_b^{\tau'} - E_b^{\tau})$ is the (variational) energy difference between the initial and final states) of the electromagnetic radiation associated with each transition as a function of the magnetic field strength B . From Fig. 5, we can see that the wavelength of the longitudinal polarized radiation in the transition $1s_0 \leftrightarrow 2p_0$ is a monotonously decreasing function of the magnetic field, reaching the domain of X-rays for $B \sim 10^{12}$ G, while the wavelength of the right polarized radiation corresponding to the transition $1s_0 \leftrightarrow 2p_{-1}$ increases for small to weak magnetic fields, reaching a maximum^v for $B \sim 0.2$ a.u. (with $\lambda_{max} \sim 1340.7$ Å), and decreasing for larger magnetic fields. Yet this transition always remains visible in the UV-region even for the stronger magnetic fields considered in the present study, $B \sim 10000$ a.u.

Figures 2, 3 and 4 show the results of the calculations for the dipole strengths, oscillator strengths and transition probabilities (formulas (6), (7) and (8) respectively) for the transitions $1s_0 \leftrightarrow 2p_{-1}$, and $1s_0 \leftrightarrow 2p_0$ in the domain of magnetic fields $B \sim 0.1 - 10000$ a.u. Tables IV and V also show the results of those quantities for magnetic fields $B = 0 - 10000$ a.u.

4. Conclusions

Throughout the present study we have used a variational approach with a physics recipe for choosing simple trial functions, as a test for an alternative method to study electromagnetic transitions in the hydrogen atom placed in a constant magnetic field. We assume that the proton is infinitely massive (Born-Oppenheimer approximation of zero order). It was found that the method yields very accurate results for the binding energies, in particular, for the lowest states studied, $1s_0, 2p_{-1}, 2p_0$, in the entire range of magnetic fields $B = 0 - 4.414 \times 10^{13}$ G. The results for binding energies show that the accuracy given by the simple 7-parametric trial functions (3),(4) and (5) is excellent for *small* magnetic fields $B \lesssim 0.1$ a.u., however it decreases monotonously as the magnetic field grows: the relative differences between the re-

sults given by the proposed trial functions (3),(4) and (5) and the most accurate results up to date Refs. 10 and 11 reach about $\sim 1\%$ for $B = 1000$ a.u. A possible explanation for this reduction in accuracy is the fact that transverse and longitudinal degrees of freedom (ρ and z respectively) in the trial functions (3), (4) and (5) appear ‘isotropically’ in the electron-proton distance r , preventing their adiabatic separation at $B \rightarrow \infty$.

Dipole $d^{(q)}(B)$, and oscillator strengths $f^{(q)}(B)$, of the electromagnetic transitions ($1s_0 \leftrightarrow 2p_{-1}$ and $1s_0 \leftrightarrow 2p_0$) were computed with the approximate wave functions (3),(4), (5) as functions of the magnetic field strength B . Our results for the $1s_0 \leftrightarrow 2p_{-1}$ transition are in very good agreement with the results of Ref. 10, with small deviations varying rather monotonously in $0.001 - 0.1\%$ for the interval of magnetic fields $B = 0.1 - 1000$ a.u. Major deviations between the present results and the results in Ref. 10 for the dipole and oscillator strengths were observed in the case of the $1s_0 \leftrightarrow 2p_0$ transition, where we have differences up to $\sim 30\%$ in the oscillator strength $f_{1s_0 \leftrightarrow 2p_0}^{(0)}(B)$ at $B = 1000$ a.u. A similar difference $\sim 30\%$ is obtained for the corresponding transition probability $w_{1s_0 \leftrightarrow 2p_0}^{(0)}(B)$. It is worth emphasizing that for a strong magnetic field $B \simeq 1000$ a.u. the transition probability $w_{1s_0 \leftrightarrow 2p_0}^{(0)}(B)$ is 3 orders of magnitude larger than the transition probability $w_{1s_0 \leftrightarrow 2p_{-1}}^{(+1)}(B)$ corresponding to the $1s_0 \leftrightarrow 2p_{-1}$ transition, so the difference in results for the transition probability $w_{1s_0 \leftrightarrow 2p_{-1}}^{(+1)}(B)$ might be of relevance for the analysis of the X-ray spectra of neutron stars.

It is important to mention that, although there is a criterion for variational binding energies to decide which results given by different approximate wavefunctions are better (since variational binding energies approach the true binding energies from below), there is no similar criterion for other expectation values or matrix elements. Thus, it is not clear so far which results for dipole strengths are better. Therefore, more investigations on the electromagnetic transitions in the hydrogen atom in a magnetic field, especially in the domain of strong magnetic fields, would be desirable in order to answer this question.

Acknowledgments

This work was supported in part by DGAPA grant PAPIIT **IN121106** (Mexico). The authors are sincerely grateful to A. Turbinger for his valuable and numerous discussions, and careful readings of the manuscript, and to D. Baye for his valuable comments and criticism regarding the present work.

i i.e. the nodal surfaces defined by the condition $\psi_{trial}(r, \theta, \phi) = 0$.

ii The binding energy is defined as the energy difference between the energy of a free electron in the magnetic field B and the

total energy E_T , i.e. $E_b = B(1 + |m| + m) - E_T$ (for states in the ground Landau-level).

iii The case of the ground state $1s_0$ was analyzed in Ref. 21 with the trial function (3). However, in order to have precise numer-

- ical information of the variational parameters appearing in the trial function, we repeated the calculations done in Ref. 21 for all the magnetic fields quoted there.
- iv* A comparison of the present results obtained in *length form* with calculations using the *velocity form* would give an estimate of the consistency in the accuracy of the presented results.
- v* Hydrogen transitions whose wavelengths go through maxima or minima as functions of the magnetic field are called *stationary lines*.
1. W. Becker and G. Pavlov, *Pulsars and isolated neutron stars*, Edited by Johan A.M. Bleeker, Johannes Geiss and Martin C.E. Huber, *The century of Space Science* Volume 1, Kluwer Academic Publishers, (2001) 721; astro-ph/208356.
 2. V.E. Zavlin, *Thermal emission from isolated neutron stars: theoretical and observational aspects* (2007); astro-ph/0702426v1.
 3. D. Sanwal, G.G. Pavlov, V.E. Zavlin and M.A. Teter, *ApJL* **574** (2002) L61; (astro-ph/0206195).
 4. M.H. van Kerkwijk *et al.*, *ApJ* **608** (2004) 432; (astro-ph/0311195).
 5. A.V. Turbiner and J.-C. Lopez Vieyra, *Mod.Phys.Lett.* **A19** (2004) 1919; (astro-ph/0404290).
 6. A. V. Turbiner, *A helium-hydrogenic molecular atmosphere of neutron star 1E1207.4-5209*, Contribution to *Physics Of Neutron Stars - 2005*, June 27 - 29, Ioffe Physico-Technical Institute, Saint-Petersburg, Russia (2005); (astro-ph/0506677).
 7. K. Mori and W.C.G. Ho, *Mon. Not. R. Astron. Soc.* **377** (2007) 905; (astro-ph/0611145).
 8. K. Mori and J.S. Heyl, *Mon. Not. R. Astron. Soc.* **376** (2007) 895; (astro-ph/0610253v2).
 9. R.H. Garstang, *Rep. Prog. Phys.* **40** (1976) 105.
 10. H. Ruder, G. Wunner, H. Herold, and F. Geyer, *Atoms in strong magnetic fields* (Springer-Verlag, 1994).
 11. Yu.P. Kravchenko, M.A. Liberman and B. Johansson, *Phys. Rev.* **A54** (1996) 287.
 12. B.M. Karnakov and V.S. Popov, *ZhETF* **124** (2003) 996; *JETP* **97** (2003) 890 (English Translation).
 13. A.V. Turbiner, *ZhETF* **79** (1980) 1719; *Soviet Phys.-JETP* **52** (1980) 868 (English Translation); *Usp. Fiz. Nauk.* **144** (1984) 35; *Sov. Phys. - Uspekhi* **27** (1984) 668 (English Translation); *Yad. Fiz.* **46** (1987) 204; *Sov. Journ. of Nucl. Phys.* **46** (1987) 125 (English Translation); Doctor of Sciences Thesis, ITEP, Moscow, 1989 (unpublished), *Analytic Methods in Strong Coupling Regime (large perturbation) in Quantum Mechanics*.
 14. I.I. Sobel'man, *Introduction To The Theory Of Atomic Spectra*, Pergamon Press Oxford - New York - Toronto - Sydney - Paris - Braunschweig, (1972).
 15. G. Wunner and H. Ruder, *ApJ* **242** (1980) 828.
 16. C. Cuveliez, D. Baye, and M. Vincke, *Phys. Rev. A* **46** (1992) 4055.
 17. G.G. Pavlov and A.Y. Potekhin, *ApJ.* **450** (1995) 883.
 18. A.Y. Potekhin, *J. Phys.* **B27** (1994) 1073.
 19. A.Y. Potekhin, *J. Phys.* **B31** (1998) 49.
 20. V.G. Bezchastnov, G.G. Pavlov and J. Ventura, *Phys. Rev.* **A58** (1998) 180.
 21. A.Y. Potekhin and A.V. Turbiner, *Phys. Rev.* **A63** (2001) 065402.
 22. A.R.P. Rau and L. Spruch, *ApJ* **207** (1976) 671.
 23. N.L. Khvingia and A.V. Turbiner, *J. Phys. B* **25** (1992) 343.
 24. H.O. Pilón, *Estudio de los estados mas bajos del átomo de higrógeno en campos magnéticos y transiciones radiativas*, MSc. Thesis (in spanish), UNAM, Mexico, (2007).